A Study of the Motion Response of Floating Solar PV and Cross-Flow Savonius Turbine in Moored Conditions

Patrick Ramsy de Fretes[1], *Mohammad* Izzuddin Jifaturrohman[2], *Teguh* Putranto[1], *I Ketu*t Aria Pria Utama[1*], and *Luofeng* Huang[3]

[1] Department of Naval Architecture, Faculty of Marine Technology, Institut Teknologi Sepuluh Nopember, Surabaya, Indonesia
[2] Department of Ocean Engineering, Faculty of Marine Technology, Institut Teknologi Sepuluh Nopember, Surabaya, Indonesia
[3] Faculty of Engineering and Applied Sciences, Cranfield University, MK 43 0AL, UK.

Abstract. The transition towards Net Zero Emissions (NZEs) is being accelerated by hybrid renewable technologies such as Floating Photovoltaic (FPV) systems and marine current turbines, which combine solar panels and cross-flow marine turbines mounted on floating structures for near-shore applications. Despite their innovative potential, these renewable technologies face significant challenges in stability and durability due to the effects of wind, waves, and ocean currents. Therefore, a flexible mooring system is essential to address these challenges. This research examines the influence of variations in the number of mooring lines and wave direction on the hydrodynamic response of FPV systems. Utilizing a catenary mooring system consisting of anchors, mooring lines, floats, and connectors, the study evaluates various configurations to determine the optimal solution for enhanced motion stability. Computational Fluid Dynamics (CFD) simulations are employed to analyze the dynamic response of FPV systems under different environmental conditions, represented on a sea-state scale, with a focus on pure oscillatory motions: heave, roll, and pitch. The findings aim to provide valuable insights for the design and operation of more stable and efficient FPV systems in marine environments, thereby supporting the advancement of sustainable renewable energy.

1 Introduction

Solar power plants, or PLTS, in Indonesia still face challenges in development, despite their potential to support the acceleration of renewable energy in the primary energy mix. One of the main obstacles is the limitation on the installed capacity of PLTS due to the surplus electricity supply experienced by PT Perusahaan Listrik Negara (Persero). Commitments and efforts to accelerate the energy transition are increasingly being made through the

* Corresponding author: kutama@na.its.ac.id

development of new, cleaner, cheaper, and more effective renewable energy technologies.One such emerging technology is Floating Photovoltaic (FPV). This system utilizes solar panels mounted on floating pontoons and placed on a water body. The FPV system uses the water's surface as the installation site for solar panel modules, exposing it to wave and wind loads [1]. The FPV system uses the water surface (water body) as the location for the installation of solar panel modules, so it will be exposed to wave and wind loads [2]. To enhance the energy output of FPV, a Cross-Flow Savonius Turbine can be added [3]. This type of turbine is a vertical-axis turbine that harnesses water currents to generate energy, differing from traditional Savonius turbines, which are typically vertical in shape. However, the implementation of this technology also faces significant challenges, particularly concerning stability. One of the main challenges is understanding and managing the hydrodynamic movements that affect these floating structures. Water movements caused by wind, waves, and ocean currents can cause dynamic forces that affect the stability and reliability of FPV systems. Therefore, it is important to analyze the hydrodynamic motion in FPVs to ensure proper design and tethering. Hydrodynamic motion analysis in FPV involves the study of the interaction between floating structures and environmental elements such as waves, currents, and winds. These movements can be categorized into six degrees of freedom: heave (up and down), sway (lateral movement), surge (longitudinal movement), roll (rotation around the longitudinal axis), pitch (rotation around the transverse axis), and yaw (rotation around the vertical axis). Each of these types of movements must be analyzed to understand how the FPV structure will react to changing environmental conditions. In order to limit the movement of floaters within the required design value, a mooring system is applied to ensure their safety and operational efficiency [4].

The system usually consists of an anchor, a mooring rope, a buoy and a connector. The catenary mooring system consists of anchors, mooring lines, buoys, and connectors [5]. Each of these components plays an important role in ensuring the stability and safety of the moored structure. The weight of the mooring rope creates a horizontal force that helps stabilize the structure against environmental forces such as wind, waves, and currents. The catenary curve ensures that most of the force is absorbed by the mooring system, thereby reducing the load on the floating structure [6].

In several projects, FPV systems designed for marine environments have begun to be developed using materials resistant to corrosion and extreme conditions in marine waters [7]. Research on FPV systems has generally focused on analyzing the aerodynamic behavior of the system, particularly for FPVs installed on inland water bodies [8] [9] [10]. However, studies on hydrodynamics remain very limited, even though such studies are crucial as they can affect energy production, system lifetime, design, stability, and safety [11] [1]. In this study, FPV with Turbine is analyzed using the BEM application. With varying wave directions, the system is tested to find optimal solutions that offer the best stability. This analysis employs computer simulations to study the dynamic responses of FPV systems under different environmental conditions.

2 Methodology

The 3D panel diffraction method, utilizing the Boundary Element Method (BEM), offers a robust numerical approach for solving linear partial differential equations formulated as integral equations. BEM is particularly effective for addressing seakeeping issues in both the frequency and time domains, accounting for both first and second-order effects. By discretizing the hull surface into small panels, the 3D-panel method accurately represents the complex geometry of a vessel [12]. Then for cable dynamics are considered to determine the forces on the cable, which vary over time, with the cable typically responding in a nonlinear manner. The solution is fully coupled, meaning that cable tensions and vessel motions are

mutually interactive. The dynamic response of the cable is computed numerically using the discrete lumped-mass method (Aqwa Theory).

The following subsection presents data on the proposed floater design, including the initial main dimensions, hydrostatic values, and an isometric view of the 3D model. It also provides a description of the mooring line properties and the arrangement for station-keeping.

2.1 Model Description & Material Properties

The dimensions and hydrostatic parameters for each proposed floater design are provided in Table 1. Furthermore, the FPV structure must be optimized to endure challenging near-shore environmental conditions while maintaining lightweight material properties to ensure economic feasibility. To achieve this, High-Density Polyethylene (HDPE) is utilized, as it offers ease of implementation and reduces the tension on the floating structure caused by hydrodynamic forces [13][14] [1]

The 3D engineering design, shown in isometric views in Figure 1 [15][3]. The design features a floating photovoltaic (FPV) structure with Cross-Flow Savonius Turbine arranged in a single-array configuration. It includes a wide service deck designed to install an array of solar panels. The hulls are connected by rigid HDPE beams, which support solar panels on each hull, all of which have identical main dimensions. The turbine design main dimension is provided in Table 1 which includes length, tension, and so on.

Table 1. Main dimension and hydrostatic properties

Parameter	Value	Units
Floating Photovoltaic (FPV)		
Lengthover All (LoA)	3,24	m
Breadth (B)	11,94	m
Height (H)	0,3	m
Draft (T)	0,12	m
Demihull Width (B1)	0,74	m
Spacing (S)	2,8	m
Turbine		
Type	Savonius turbine	
Height *(H)*	0,16	m
Diameter *(D)*	0,26	m
Number of Blades *(N)*	3	
Blade Length *(d)*	0,14	m
Blade Thickness *(de)*	0,0015	m
Overlap Distance *(ds)*	0,014	m
Aspect Ratio (AR = *H/D*)	0,61	
Overlap Ratio (OR = *ds/D*)	0,05	

Parameter	AQWA	Baseline Calculation	Difference (%)
Displacement Δ (ton)	1207,89	1211,52	0,3%

Water Plane area (m^2)	9,67	9,67	0%
Longitudinal center of Gravity, LCG (m) from AP - CL	1,62	1,62	0%

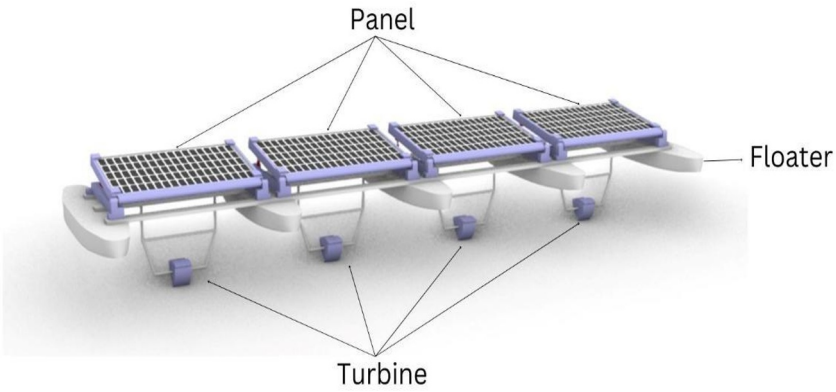

Fig 1. Isometric view of novel design in single array FPV

2.2 Mooring Properties

The Catenary mooring system arrangement is depicted in Figure 6, consisting of four mooring lines attached at the corners of the floater. The fairlead locations are positioned at the outer edges of the pentamaran floater system, aligned with the water surface elevation (draft). The mooring configuration consider a 45-degree angle relative to the global Y-axis and utilizes a catenary-type mooring system. A water depth of 22 meters is considered, representing nearshore conditions as depicted.

Additionally, the primary coordinates for modeling the catenary mooring configuration are presented in Table 2, which specifies the locations of the fairlead and anchor points. Table 3 further provides essential parameters relevant to the inelastic-static catenary mooring calculations.

Table 2. Anchor & Fairlead Position

Point	X	Y	Z
Anchor Position			
Anchor Fore Right	375.52	-378.06	-22.00
Anchor Fore Left	375.52	378.06	-22.00
Anchor Aft Right	-372.28	-378.06	-22.00
Anchor Aft Left	-372.28	378.06	-22.00
Fairlead Position			
Mooring Fore Right	3.19	-5.73	0.12
Mooring Fore Left	3.19	5.73	0.12
Mooring Aft Right	0.05	-5.73	0.12
Mooring Aft Left	0.05	5.73	0.12

Table 3. Mooring Properties & Catenary Cable Calculation

Parameter	Symbol	Value	Unit
Mooring Properties			
Type Mooring		6 X 19 IWRC (Independent Wire Rope Core)	

Nominal Diameter	Ø	16	mm
Nominal Strength	MBL	16.2	MT
Approx Mass In Air	Wa	1.55	Kg/m
Parameter	**Symbol**	**Value**	**Unit**
Modulus Young	E	113000000	kN/m^2
Fill Factor	F	0.57	
Gross Cross Sectional Area	Ag	2.01E-04	m^2
Nett Cross Sectional Area	An	1.15E-04	m^2
Axial Stiffness	EA	1.30E+04	kN
Inelastic-Static Catenary Cable Calculation			
Static Horizontal Tension	T_H	0.70	MT
Allowable Tension Max	$T_{a\text{-}max}$	8.53	MT
Submerged Weight	Ws	1.34	kg/m
Water Depth	h	22.00	m
Ratio Between T_H and Ws	a	524.49	m
Catenary Length	ls	153.50	m
Catenary Weight	Ws*h	29.54	kg
Minimum Length of the Wire Rope	l_{min}	528.14	m
Horizontal Catenary	x	151.91	m
Touchdown	xt	374.64	m
Horizontal Distance	X	526.55	m

The computation of pressures and forces acting on each discretized numerical element of the hull surface geometry is derived from the mesh generated within the diffraction system (Bosma et al., 2012). A high-resolution mesh with total elements 20840 and total nodes 21324 was utilized across the entire surface of the FPV models, as demonstrated in Figure 2.

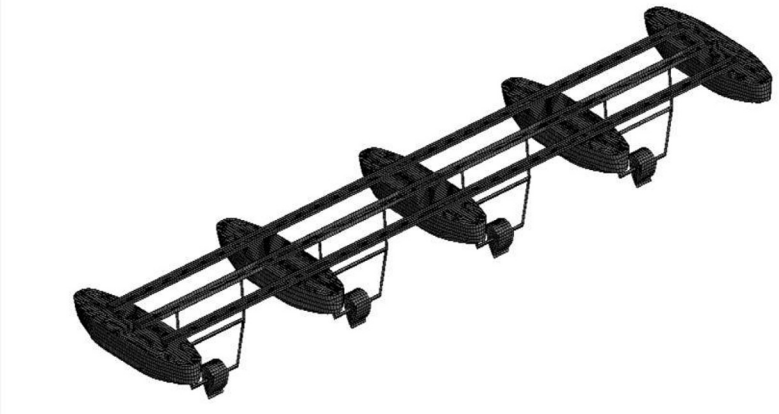

Fig 2. Pentamaran mesh visualization

3 Result & Discussion

The results and discussion section of this study is divided into several focused subsections. It first addresses the motion transfer functions for each mode, comparing the behaviors under free-floating and moored conditions. This is followed by an analysis of the wave spectral density energy, covering a wave frequency spectrum from ω = 0.05 rad/s to 5.00 rad/s. Additionally, water elevation data obtained from the numerical simulations is presented. A

comprehensive time-dependent evaluation was conducted over a simulation period of 10,800 seconds to capture the dynamic motion responses of the pentamaran floater under moored conditions, accounting for the combined effects of waves, currents, and wind forces. Lastly, the study includes an assessment of mooring cable tensions for various wave headings to evaluate the hydrodynamic forces influencing the axial loads on the cables.

The dynamic behaviour of FPV structures under hydrodynamic loads is analyzed by considering wave propagation scenarios, including head seas (φ = 0°), quartering seas (φ = 45°), and beam seas (φ = 90°). Environmental loads impacting the FPV structure are evaluated under both collinear and omnidirectional conditions for all wave headings[16].

3.1 Comparison Between Pentamaran With Turbine & Without Turbine

This subsection discusses the comparison between turbines and turbinesless structures in 3 movements: Heave, Roll, and Pitch.

3.1.1 Heave (Global Z)

At low frequencies, the turbine does not exert a significant influence on the movement of the FPV, as the RAO value remains close to 1, indicating that the FPV is still following the movement of the waves completely. However, at medium to high frequencies, FPV provide effective damping of FPV movements. The RAO value for conditions with turbine is lower than without turbine, which means that the amplitude of the FPV heave movement is reduced. This shows that turbine play an important role in improving the motion of FPV, especially in short-wave and fast wave conditions. The graph shows that the presence of the turbine has a minor influence on the structure's response in the heave direction, as indicated by the small differences between the two curves, particularly at higher wave frequencies. This can be observed in Fig 3.

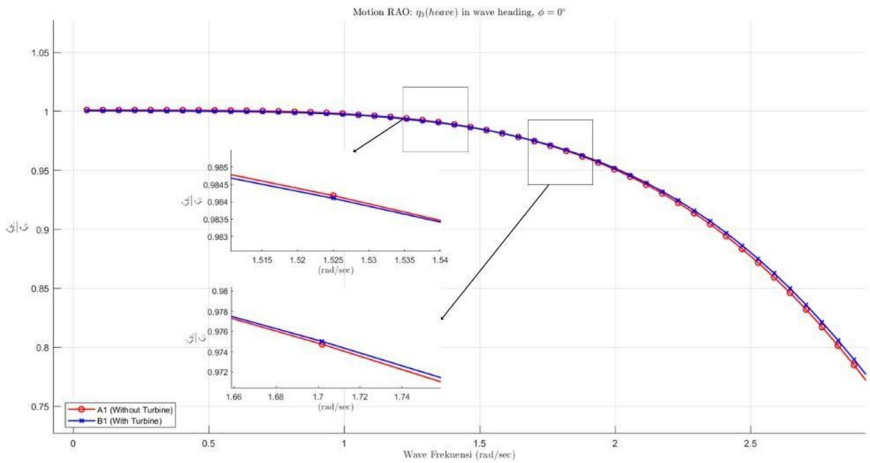

(a)

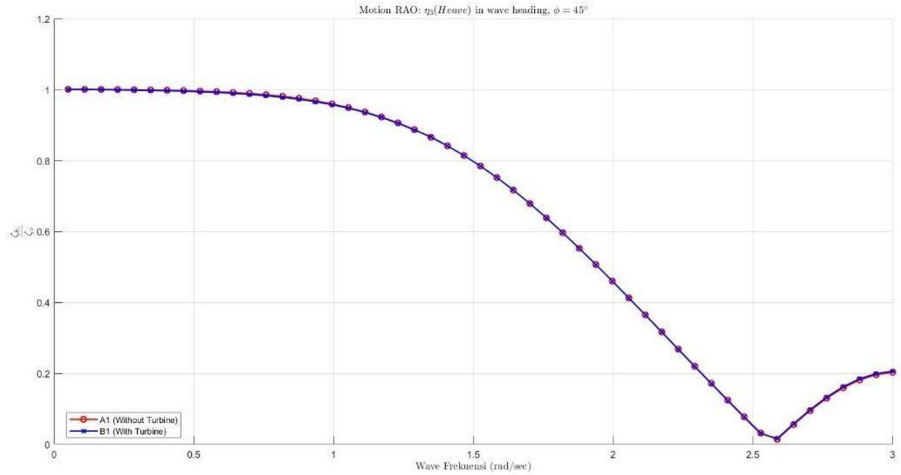

(b)

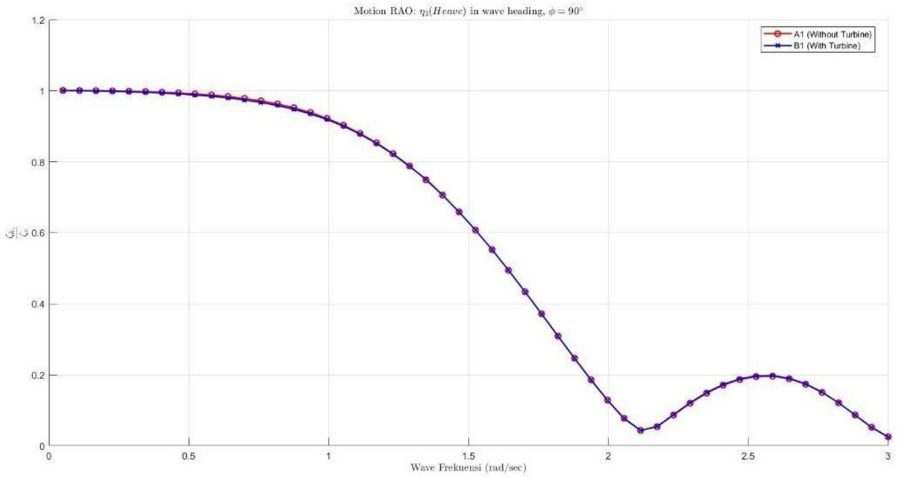

(c)

Fig 3. Response RAO Heave (Global Z) pentamaran FPV with turbine and without turbine: (a) 0 dg; (b) 45 dg; (c) 90 dg

The graph shows that the presence of the turbine has a minor influence on the structure's response in the heave direction, as indicated by the small differences between the two curves, particularly at higher wave frequencies. This can be observed in Figure 3.

3.1.2 Roll (Global RX)

The addition of turbine significantly impacts roll motion, particularly at resonance frequencies where the roll amplitude becomes extremely large (around 1.5 rad/sec). While the turbine effectively dampens roll motion at high frequencies, enhancing the FPV dynamic stability in short-wave conditions, it increases susceptibility to roll resonance at mid-range

frequencies. This highlights the need for careful design adjustments or additional stabilizers to mitigate resonance effects.

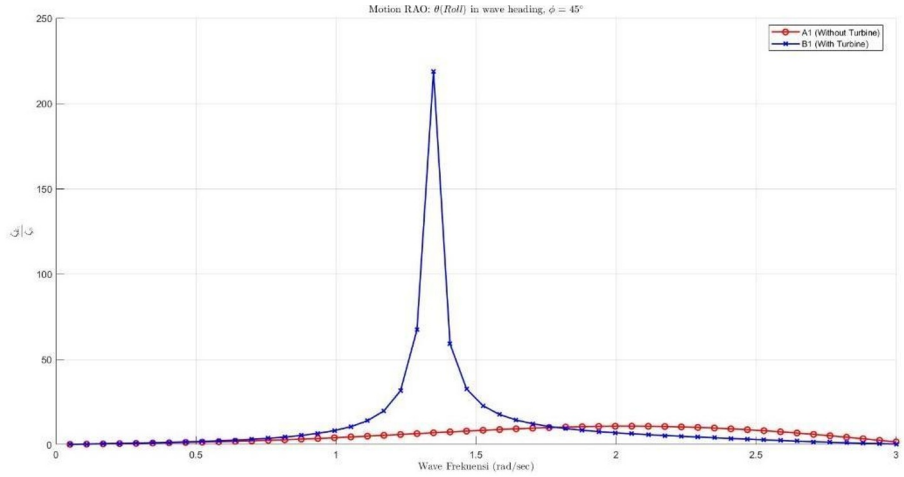

(a)

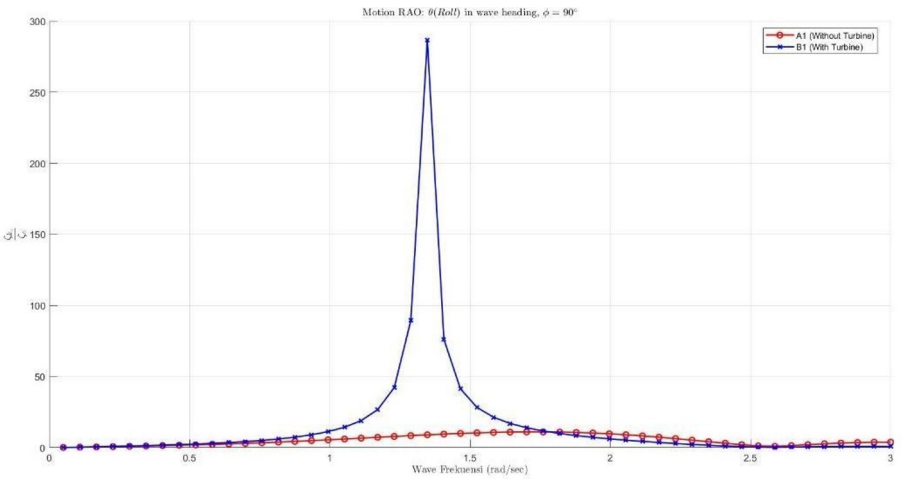

(b)

Fig 4. Response RAO Roll (Global RX) pentamaran FPV with turbine and without turbine: (a) 45 dg; (b) 90 dg

Figure 4 shows the sharp peak near 1 rad/s indicates that the wave frequency at this point closely matches the natural frequency of the system after the turbine was added. At this resonance frequency, the wave energy is highly effective in driving the roll motion, resulting in a high RAO value. In contrast, the response without the turbine (A1) remains relatively constant and much lower across all wave frequencies

3.1.3 Pitch (Global RY)

The addition of turbine increases the amplitude of pitch motion at medium to high frequencies, particularly in short-wave conditions. While it has minimal impact at low

frequencies, the increased pitch sensitivity at higher frequencies highlights the need for careful design considerations to prevent excessive pitch responses.

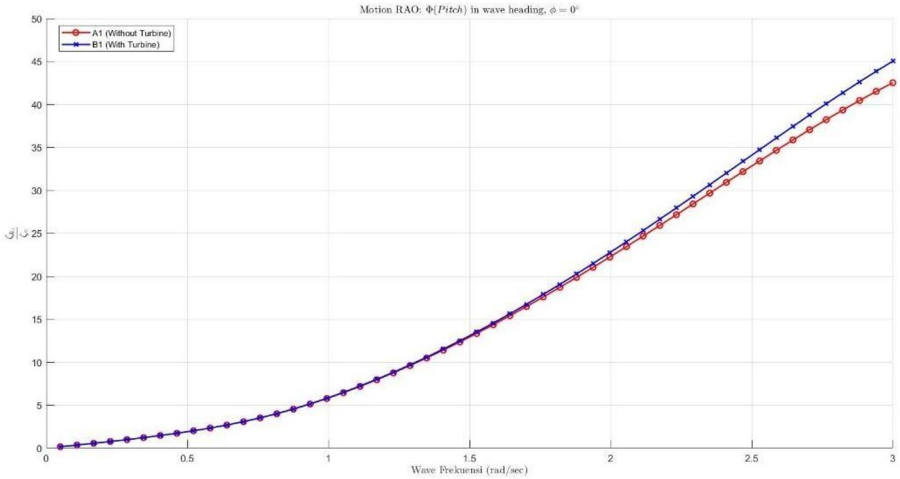

(a)

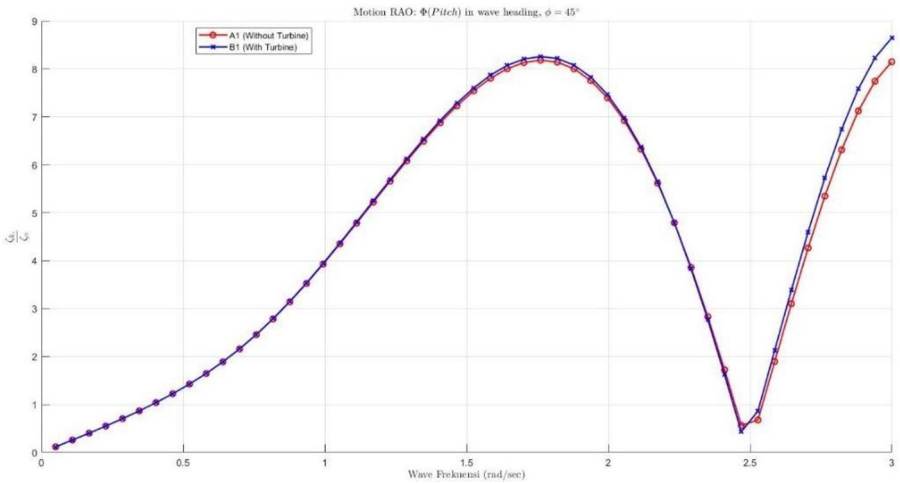

(b)

Fig 5. Response RAO Roll (Global RX) pentamaran FPV with turbine and without turbine: (a) 0 dg; (b) 45 dg

Figure 5. ilustrate both curves show an increasing trend in RAO values as the wave frequency increases. This increase is more noticeable at higher wave frequencies, where the difference between the two curves becomes more pronounced.

3.2 Time Domain Responses

This subsection discusses the time-domain responses specifically for the motions that require external restoring forces or moments to limit the displacement of the FPV structure, relying on the stiffness of the mooring cables – then called the horizontal motion. The horizontal motion quality will be evaluated over a simulation period of 3 hours to capture the coupled dynamic effects between the structure and the mooring system.

3.2.1 Horizontal Responses

Figure 6 illustrates the motion quality of the FPV structure under moored conditions for surge, sway, and yaw motion modes.

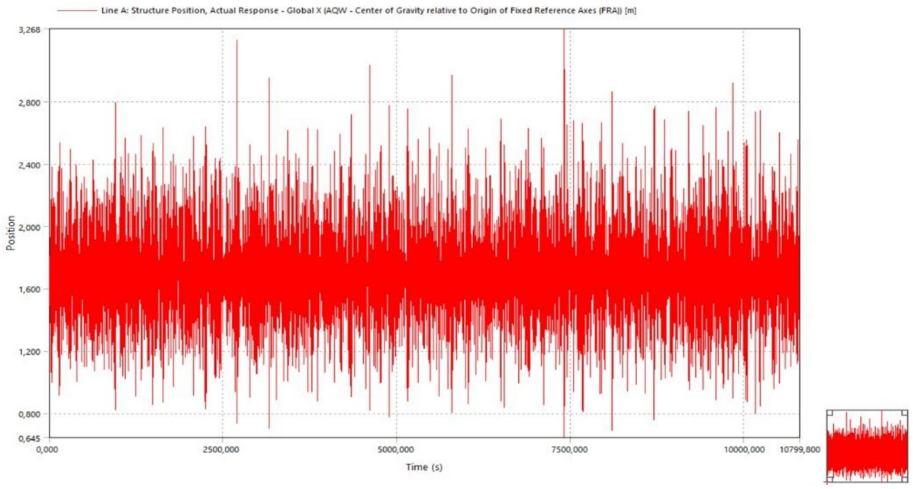

(a)

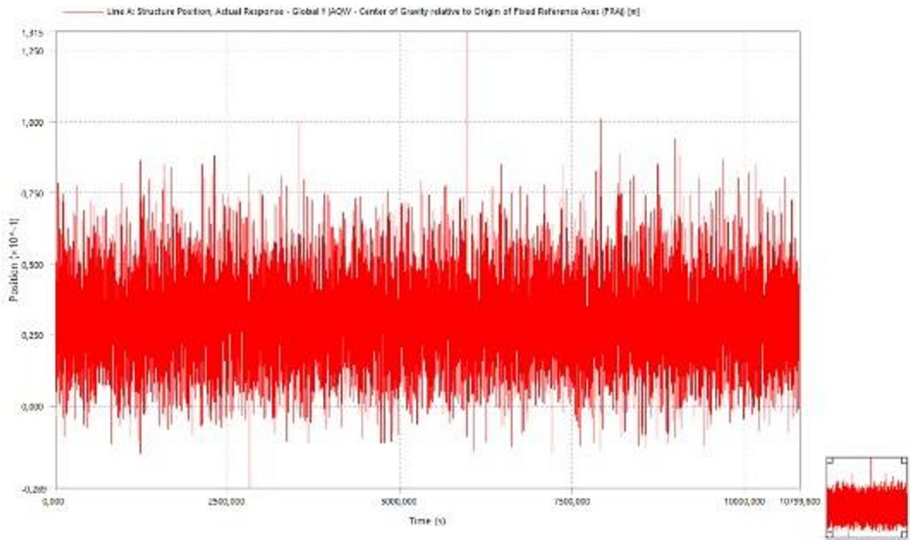

(b)

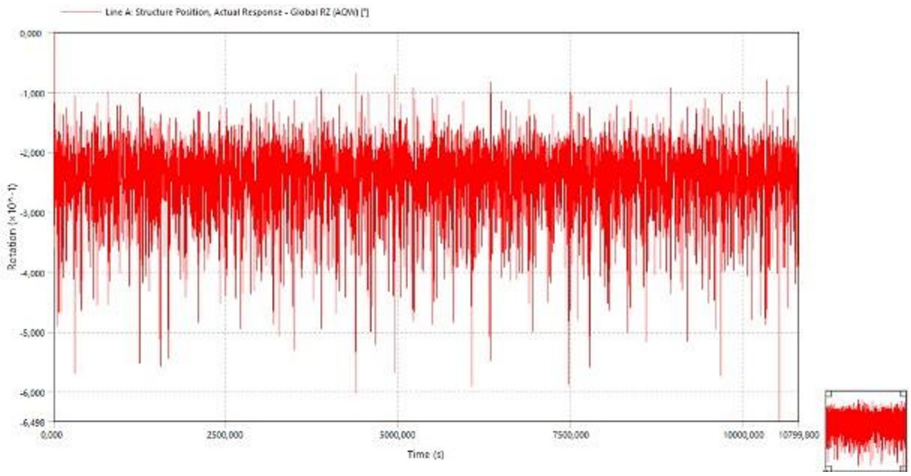

(c)

Fig 6. Time domain responses for pentamaran FPV with turbine: (a) Surge (0 dg) min. Value 0,64 m & max. Value 3,26 m; (b) Sway (90 dg) min. Value -0,02 m & max. Value 0,13 m; (c) Yaw (45 dg) min. Value -0,6 dg & max. Value 0 dg

3.3 Time Domain Cable Tension

This subsection concludes by discussing the time-domain analysis of cable tension for each mooring cable in the single-array pentamaran FPV structure. The configuration consists of four mooring cables arranged at 45° angles relative to the global Y-axis. Similar to the motion response analysis, the cable tension evaluation is conducted over a 3-hour simulation period to capture dynamic effects caused by wind, waves, and currents.

Figure 7 presents a 3D surface diagram illustrating the cable tensions for various environmental loading directions: 0°, 45°, and 90°.

- φ = 0° Loading Direction: Cable 4 experiences the highest tension, reaching approximately 19,89 kN, while Cable 1 shows the lowest tension, around 1,23 kN.
- φ = 45° Loading Direction: Cable 4 exhibits the maximum tension at 11,83 kN, whereas Cable 2 has the lowest tension at 6,58 kN.
- φ = 90° Loading Direction: Cable 4 records the highest tension at 10,23 kN, while Cables 2 and 3 share the lowest tension at approximately 8,08 kN

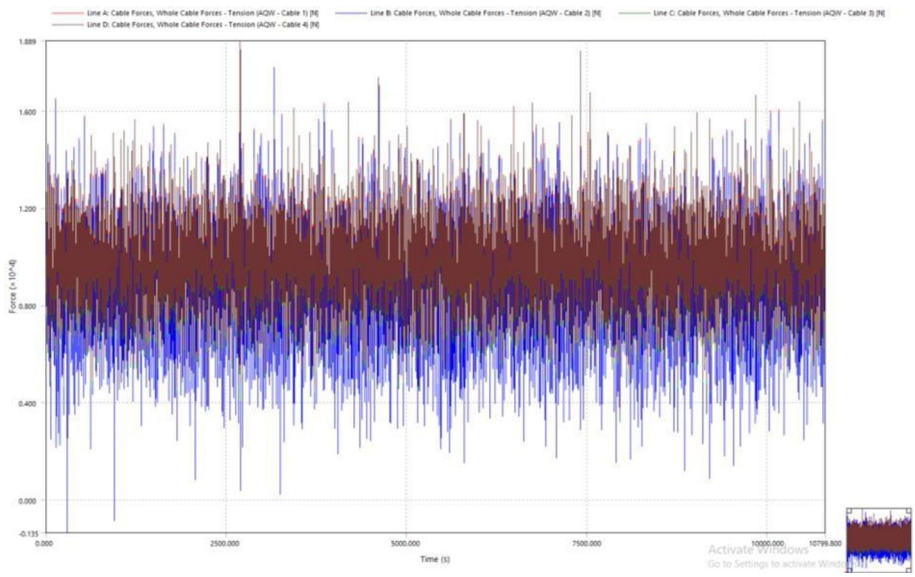
Line A: Cable Forces, Whole Cable Forces - Tension (AQW - Cable 1) [N]
Line B: Cable Forces, Whole Cable Forces - Tension (AQW - Cable 2) [N]
Line C: Cable Forces, Whole Cable Forces - Tension (AQW - Cable 3) [N]
Line D: Cable Forces, Whole Cable Forces - Tension (AQW - Cable 4) [N]
1.889
1.600
1.200
0.800
0.400
0.000
-0.135
Force (x 10^4)
0.000
2500.000
5000.000
7500.000
10000.000
10799.800
Time (s)

(a)

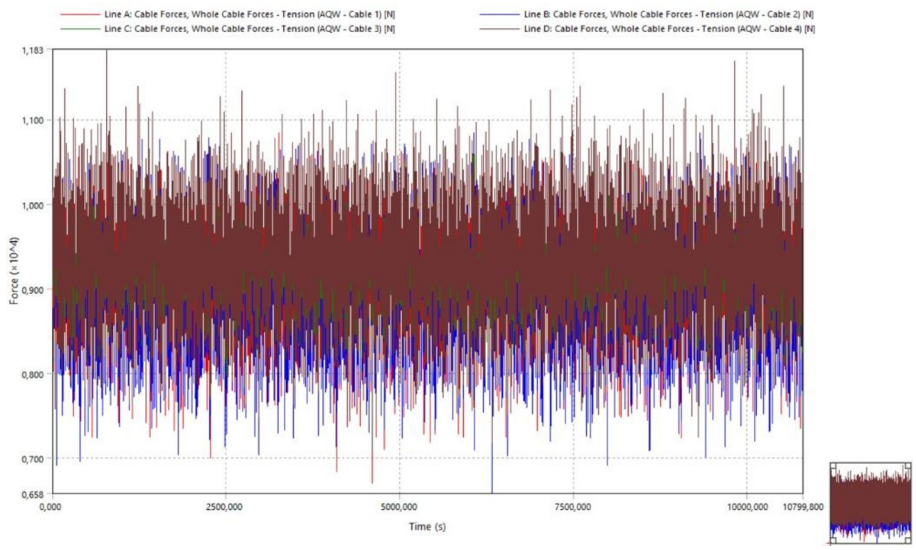
Line A: Cable Forces, Whole Cable Forces - Tension (AQW - Cable 1) [N]
Line B: Cable Forces, Whole Cable Forces - Tension (AQW - Cable 2) [N]
Line C: Cable Forces, Whole Cable Forces - Tension (AQW - Cable 3) [N]
Line D: Cable Forces, Whole Cable Forces - Tension (AQW - Cable 4) [N]
1,183
1,100
1,000
0,900
0,800
0,700
0,658
Force (x 10^4)
0,000
2500,000
5000,000
7500,000
10000,000
10799,800
Time (s)

(b)

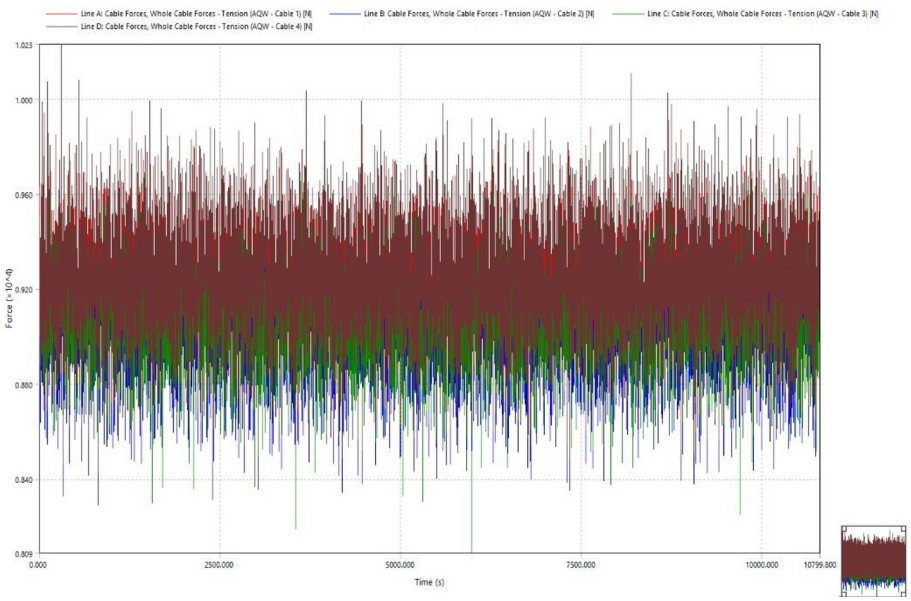

(c)

Fig 7. Maximum cable tension for pentamaran FPV with turbine: (a) 0 dg; (b) 90 dg; (c) 45 dg

4 Conclusion

This study demonstrates that platform configuration and wave conditions significantly influence the motion behavior of FPV structures and Cross-Flow Savonius Turbines in water. In the analysis of oscillatory motions, Heave and Pitch movements showed consistent patterns both with and without the presence of turbines, while Roll motion exhibited a notable increase at specific wave frequencies (1 to 1.7 Hz).

In the time-domain response analysis, the RAO amplitude varied across different motion types (Sway, Yaw, Heave), reflecting the complex dynamics of the structure influenced by platform configuration and wave interaction.

The analysis of cable tension distribution revealed that the inclination angle significantly affects system stability. At 0 degrees, tension fluctuations were high, with shifts between tensile and compressive forces, indicating instability. Stability improved at 45 degrees, where the force distribution became more balanced. At 90 degrees, the system achieved the highest stability, with the most uniform force distribution.

This study concludes that increasing the cable inclination angle enhances system stability, with 90 degrees providing the most balanced and stable configuration. These findings highlight the importance of optimizing the angle settings to improve the performance and stability of FPV structures and Savonius turbines in marine environments.

Acknowledgement

The research scheme is financed by Internal fund from Institut Teknologi Sepuluh Nopember (ITS) . The funding is disbursed through the PRIME ENGINEERING SEED FUND for the 2024/2025, Batch 2, with contract number 2502/PKS/ITS/2024. The authors would like to express their gratitude to both institutions (LPDP and ITS).

References

1. T. Reindl, "Where Sun Meets Water FLOATING SOLAR HANDBOOK FOR PRACTITIONERS," 2019. [Online]. https://www.worldbank.org
2. Z. Tajali and M. Shafieefar, "Hydrodynamic analysis of multi-body floating piers under wave action," Ocean Engineering, vol. 38, no. 17–18, pp. 1925–1933, 2011, https://doi.org/10.1016/j.oceaneng.2011.09.025.
3. D. Satrio, F. Y. Muhammad, Mukhtasor, S. Rahmawati, S. Junianto, and S. Musabikha, "Numerical simulation of cross-flow Savonius turbine for locations with low current velocity in Indonesia," Aug. 01, 2022, Springer Science and Business Media Deutschland GmbH. https://doi.org/10.1007/s40430-022-03620-w.
4. S. Rui et al., "A review on mooring lines and anchors of floating marine structures," Renewable and Sustainable Energy Reviews, vol. 199, p. 114547, Jul. 2024. https://doi.org/10.1016/j.rser.2024.114547.
5. W. Cui, S. Fu, and Z. Hu, Encyclopedia of Ocean Engineering. Springer Nature, 2022. https://doi.org/10.1007/978-981-10-6946-8.
6. "Faltinsen - 1990 - Sea loads on ships and offshore structures".
7. D. Friel, M. Karimirad, T. Whittaker, and J. Doran, "Hydrodynamic investigation of design parameters for a cylindrical type floating solar system," in Developments in Renewable Energies Offshore, CRC Press, 2020, pp. 763–770. https://doi.org/10.1201/9781003134572-87.
8. G.-H. Lee, J.-W. Choi, J.-H. Seo, and H. Ha, "Comparative Study of Effect of Wind and Wave Load on Floating PV: Computational Simulation and Design Method," Journal of the Korean Society of Manufacturing Process Engineers, vol. 18, no. 11, pp. 9–17, Nov. 2019, https://doi.org/10.14775/ksmpe.2019.18.11.009.
9. P. D. I. Torino, "POLITECNICO DI TORINO Floating photovoltaic systems: state of art, feasibility study in Florida and computational fluid dynamic analysis on hurricane resistance," 2020.
10. R.-Y. Yang and S.-H. Yu, "A Study on a Floating Solar Energy System Applied in an Intertidal Zone," Energies (Basel), vol. 14, no. 22, 2021, https://doi.org/10.3390/en14227789
11. M. Baghfalaki, S. K. Das, And S. N. Das, "Analytical Model To Determine Response Amplitude Operator Of A Floating Body For Coupled Roll And Yaw Motions And Frequency-Based Analysis," Int J Appl Mech, vol. 04, no. 04, p. 1250044, 2012. https://doi.org/10.1142/S1758825112500445.
12. B. Lagemann, "Efficient seakeeping performance predictions with CFD."
13. R. Claus and M. López, "Key issues in the design of floating photovoltaic structures for the marine environment," Renewable and Sustainable Energy Reviews, vol. 164, p. 112502, 2022.https:/doi.org/10.1016/j.rser.2022.112502.
14. S. Oliveira-Pinto and J. Stokkermans, "Marine floating solar plants: An overview of potential, challenges and feasibility," Dec. 01, 2020, ICE Publishing. https://doi.org/10.1680/jmaen.2020.10.

15. M. I. Jifaturrohman, T. Putranto, I. K. A. P. Utama, and L. Huang, “Effect of Platform Configurations and Environmental Conditions on the Performance of Floating Solar Photovoltaic Structures,” International Marine Design Conference, May 2024. https://doi.org/10.59490/imdc.2024.854.
16. E. V. . Lewis, Principles of naval architecture. Society of Naval Architects and Marine Engineers, 1989.